

# Adaptive Neuro-Fuzzy Controller for High Temperature Gas Cooled Reactor

Kushal Dinkar Badgujar, Woldesemayat Muluneh Lemma

**Abstract**—A Neuro-Fuzzy controller is applied to control the power of a high temperature pebble bed reactor (HTPBR). A simplified model of the reactor and lumped model of heat transfer is developed and used. Xenon feedback with Xenon and Iodine balance equations and feedback with power coefficient of reactivity are included. The inputs to controller are represented using seven fuzzy sets. The output is obtained as linear combinations of the inputs. Simulations were conducted for the case of reducing the reactor power from rated value at 100% to 20% and for the case of raising reactor power from 20% to 100% linearly. In these simulations, the proposed design for controller exhibits faster and more accurate response than conventional controller.

**Index Terms**— ANFIS controller, Fuzzy logic, GEN IV reactors, Reactor power control.

## NOMENCLATURE

P	Fission power	W
$\beta_i$	Delayed neutron fraction	
$\beta$	Sum of delayed neutron fraction	
$\lambda_i$	Decay constant of delayed Precursors of group i	$s^{-1}$
$C_i$	Concentration of delayed precursors of group i	Atoms $\cdot$ $m^{-3}$
$\Lambda$	Prompt neutron life time	s
$\mu$	Membership	
x	Fuzzy member	
$\rho$	Total reactivity	
$\rho_f$	Feedback reactivity	
$\rho_{ex}$	External reactivity	
$\rho_{xe}$	Feedback Xenon reactivity	
$\rho_p$	Feedback reactivity arising from power change	
Yc	Control rod speed	$ms^{-1}$
W	Reactivity worth of the rod per unit length	$\$ \cdot m^{-1}$
$K_{pw}$	Power coefficient of reactivity	$\$ \cdot W^{-1}$
$\gamma$	Static power coefficient of reactivity	$\$ \cdot W^{-1}$
I	Iodine concentration	Atoms $\cdot$ $m^{-3}$
$X_e$	Xenon concentration	Atoms $\cdot$ $m^{-3}$

## I. INTRODUCTION

The control system is considered as the most important subsystem to control spontaneous fission reaction in a nuclear reactor. The control system should maintain maximum power output of nuclear reactor with minimum static error, and should possess certain stability margin, suitable overshoot and transient time. The high temperature pebble bed reactor (HTPBR) is classified under *high temperature gas cooled reactors* (HTGR) in the GEN IV reactors family. HTGR is one of the six types of GEN IV reactors that are being developed internationally with emphasis on features like inherent safety, nuclear proliferation resistance and high thermal to electric conversion efficiency. Interesting features of HTPBR are, its enhanced efficiency without losing the advantage of high outlet temperature (1000°C) and its possible application as process heat source for chemical plants. Also the reactor uses TRISO (Tristructural-isotropic) particles as fuel element. Fuzzy logic offers better control than conventional control methods. It can execute quickly which is useful to develop real-time control system. The fuzzy logic was extended to nuclear industry by Ruan [1], [2]. Also, Adda *et al.* [3] developed the two fuzzy logic controllers to control power of a reactor accounting for temperature coefficient of reactivity. Liu *et al.* used fuzzy logic and genetic algorithm to design PID controller [4]. A simulation for near optimal linear regulator has been used to solve the control xenon-induced oscillations [5]. This method has been used to solve control problem for PHWR but it accounts only for Xenon poisoning and neglects temperature feedbacks. Power stabilization of nuclear research reactor using Fuzzy Controller has been presented by H.M. Emara and A. Elsadat *et al.* [6]. In these simulations, the adaptive fuzzy controller gave the best integral square error (ISE) index, whereas the static fuzzy controller still provided a better ISE than the conventional PD controller. Recently, a Fuzzy like PD controller for spatial control of AHWR is developed [7]. Adaptive neuro fuzzy controller has been used to control water level of steam generator of nuclear plant [8]. One of the method for controlling the plant with time varying parameter is STR [9]. This article presents a method to control power of HTPBR by using an adaptive Neuro-Fuzzy controller. A simplified reactor model with a point kinetics equation and the reactor heat balance equation is used. The reactivity feedback arising from power coefficient of reactivity, and Xenon poisoning are also considered. The reactor is operated at various power levels by using Neuro-Fuzzy controller

**Manuscript Received on February 16, 2015.**

**Kushal Dinkar Badgujar**, Division of Advanced Nuclear Engineering, Pohang University of Science and Technology, Pohang 790-784, South Korea, Korea.

**Woldesemayat Muluneh Lemma**, Department of Electrical Engineering, Pohang University of Science and Technology, Pohang 790-784, South Korea, Korea.

## II. HTPBR MODEL

Extensive model of HTPBR is given in [11,12,13] and the same has been used here for the study accomplished in this paper. However, for brevity the model is discussed briefly in the following.

### A. TRISO Fuel

The fuel particle, commonly about 1 mm in diameter, consists of a fuel kernel, typically (UO<sub>2</sub>) or Uranium oxy-carbide (UCO), surrounded by a low density pyrolytic carbon (PyC) buffer layer, and followed by structural coating of triple layered composite material consisting of silicon carbide layer (SiC) sandwich between dense PyC layers, termed inner PyC layer (IPyC) and outer PyC layer (OPyC). The resulting particle is called a TRISO fuel particle. Triple layered coating around fuel kernel acts as barrier for fission products released. TRISO particles are embedded in spherical graphite fuel known as pebbles (Fig. 1).

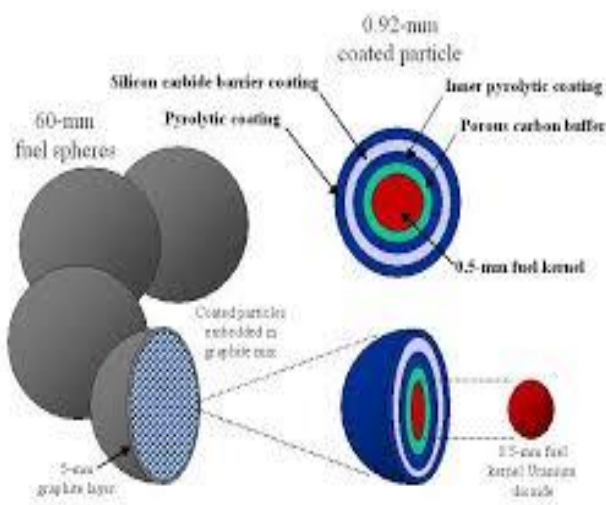


Fig. 1. Schematic of TRISO particles and pebbles in HTPBR [10]

A pebble is 6 cm in diameter and contains ~ 15000 coated particles within the graphite matrix.

### B. Reactor Core

A typical 120-MWe reactor core design uses ~ 36000 pebbles. The pebbles are circulated in the reactor. Partially burned and fresh fuel, when necessary, is added to the top core which has geometry similar to that of a fluidized packed bed. Fuel pebbles then flow down through the core region. Upon exiting the core after a particular pass, the pebbles are checked for accumulated burn-up and integrity. Based on the results of this analysis a pebble is either removed from the stream and a new one is added, or it is recycled by adding to the top (entrance) of the core. Heat is transferred from the fuel, usually to, the helium flowing through the core. The HTPBR is in the form of a cylinder. In the present work, the core is represented by concentric cylindrical rings. The graphite pebbles are at the center of the core and act as reflector. The core is symmetric about an inner graphite reflector. Each ring has 12 vertical divisions (Fig. 2).

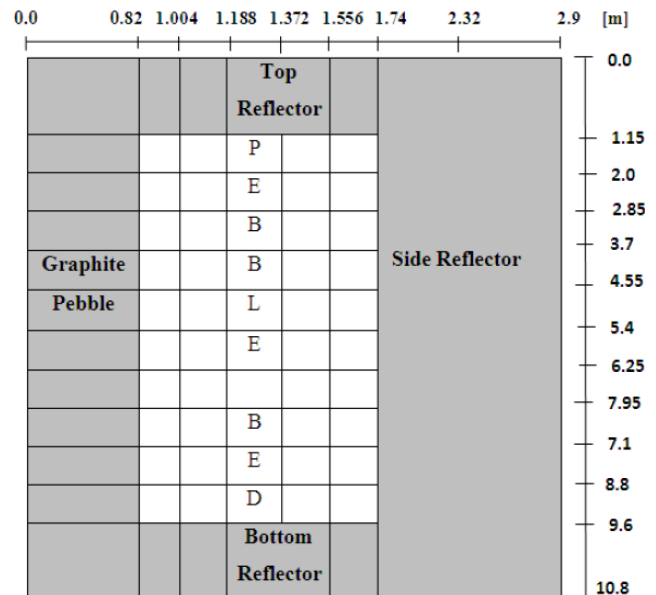


Fig. 2. Schematic of in HTPBR [10]

In the steady state, and in the transient state the normalized fission power distribution holds good. The axial power distribution from top to bottom of the core is [0.025 0.034 0.053 0.071 0.121 0.148 0.171 0.162 0.124] whereas power distribution from inner ring to outer ring in the active region is [0.218 0.0207 0.195 0.19 0.19]. This power distribution is used to calculate power coefficient of reactivity.

## III. CONTROLLER MODEL

The error signal between reactor power and external demand is fed to proportional controller and derivative controller with gains  $K_p$  and  $K_d$  respectively (Fig. 3). The output signal of Adaptive Neuro-Fuzzy controller indicates the velocity of the control rod.

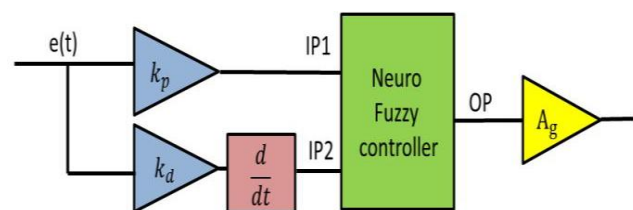


Fig. 3. Adaptive neuro fuzzy controller

In Neuro-Fuzzy controller, the linear combination of the inputs (weighted sum) is performed. This is further attenuated to obtain the overall output.

## IV. GOVERNING EQUATIONS

For the transient analysis, following set of differential equations are solved. Reactor power variation is obtained by solving the following seven point-kinetics equation.

$$\frac{dp(t)}{dt} = \frac{\rho - \beta}{\Lambda} p(t) + \sum_{i=1}^6 \lambda_i C_i \quad (1)$$

$$\frac{dC_i(t)}{dt} = \frac{\beta_i}{\Lambda} p(t) - \lambda_i C_i (i = 1, 2, \dots, 6) \quad (2)$$

The prompt-neutron life time  $\Lambda$  is  $4.0 \times 10^{-5}$  s for HTPBR and effective delayed-neutron fraction  $\beta$  is  $\sum_{i=1}^6 \beta_i$ . The method for determining the power coefficient of reactivity for HTPBR has been presented by Badgujar et al. [10]. The power coefficient of reactivity is defined as ratio of reactivity change to power change, and is calculated for the reactor model described earlier by using the ratio of temperature change of fuel to the corresponding power change. The energy conservation principle is used to calculate the fuel temperature. The kinetic model used for HTPBR has been shown in Fig.4. The reactivity is the sum of internal feedback reactivity and external reactivity. The following equations are used to obtain transient analysis.

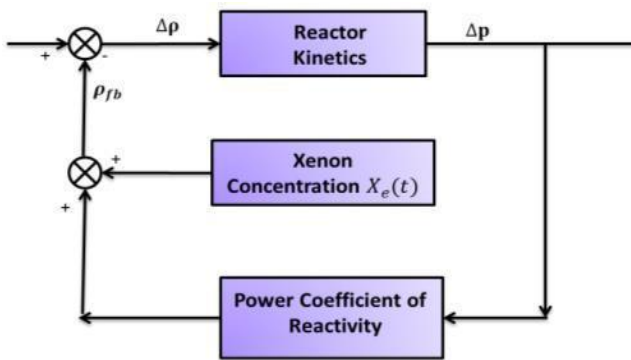


Fig. 4. Kinetic model for HTPBR

$$\rho = \rho_{ex} + \rho_{xe} + \rho_p, \quad (3)$$

$$\frac{d\rho_{ex}}{dt} = Y_c \times W, \quad (4)$$

$$\Delta\rho_p(s) = K_p(s)\Delta P(s), \quad (5)$$

$$K_p(s) = \frac{\gamma}{1 + s\tau}, \quad (6)$$

$$\rho_{xe} = \frac{-\Sigma_a X}{v\Sigma_a}, \quad (7)$$

$$\frac{dI}{dt} = \gamma_I \Sigma_f \phi(t) - \lambda_I I, \quad (8)$$

$$\frac{dX}{dt} = \lambda_I I + \gamma_X \Sigma_f \phi(t) - (\lambda_X I + \sigma_a^X \Phi) X, \quad (9)$$

where,

- $\Sigma_a$  is macroscopic absorption cross section in fuel.
- $\sigma_a^X$  is microscopic absorption cross section in xenon.
- $\phi$  is space averaged flux.

The constant values used in the simulation are enlisted in the Table I.

TABLE I  
VALUES OF CONSTANT PARAMETERS

Parameter	Value
$\beta$	0.0065
$\Lambda$	$4.0 \times 10^{-5}$
$\lambda_x$	0.00237
$\gamma_x$	$2.09 \times 10^{-5}$
$\lambda_I$	0.0639
$\gamma_I$	$2.87 \times 10^{-5}$

$\Sigma_f$	197.7328 at 8% Enrichment
$\sigma_a^x$	$2.65 \times 10^6$
$\nu$	2.42
$k_p$	0.5
$k_d$	0.01
$\emptyset$	$10^{14}$

## V. METHOD

The inputs to the Neuro-Fuzzy controller are represented by fuzzy sets. Each fuzzy set consist of elements and their associated membership. Membership varies depending upon type of membership function used. In this paper, we use combination of trapezoidal and triangular membership functions (Fig. 5).

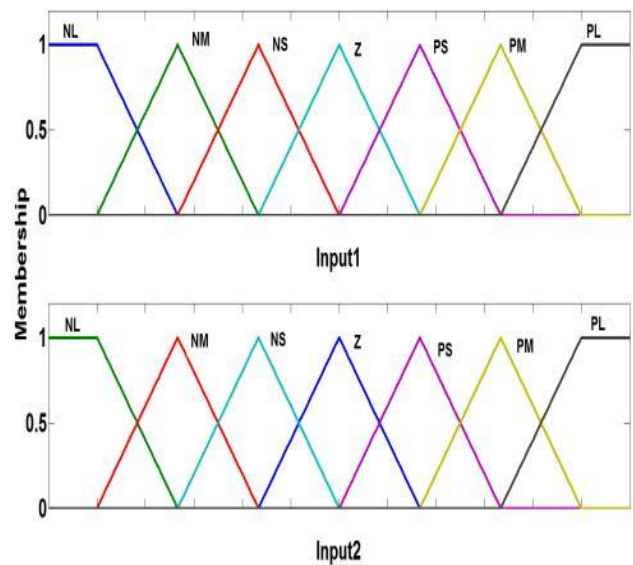


Fig. 5. Membership function for Input1 and Input2

The generalized expression for a trapezoidal membership can be written in general as,

$$\mu_A(x) = \begin{cases} 0 & x \leq a_A, \\ \frac{x - a_A}{b_A - c_A} & a_A \leq x \leq b_A, \\ 1 & b_A \leq x \leq c_A, \\ \frac{d_A - x}{d_A - c_A} & c_A \leq x \leq d_A, \\ 0 & x \geq d, \end{cases} \quad (10)$$

where  $[a_A \ b_A \ c_A \ d_A]$  are the four parameters of the trapezoidal membership function. The expression for the triangular membership function is given as,

$$\mu_A(x) = \begin{cases} 0 & x \leq a_A, \\ \frac{x - a_A}{b_A - a_A} & a_A \leq x \leq b_A, \\ \frac{c_A - x}{c_A - b_A} & b_A \leq x \leq c_A, \\ 0 & c_A \geq x. \end{cases} \quad (11)$$

where  $[a_A \ b_A \ c_A]$  are the three parameters of the trapezoidal membership function. The structure of the Neuro-Fuzzy controller has five layers (Fig.6).  $O_{l,i}$  is the output of the  $i^{th}$

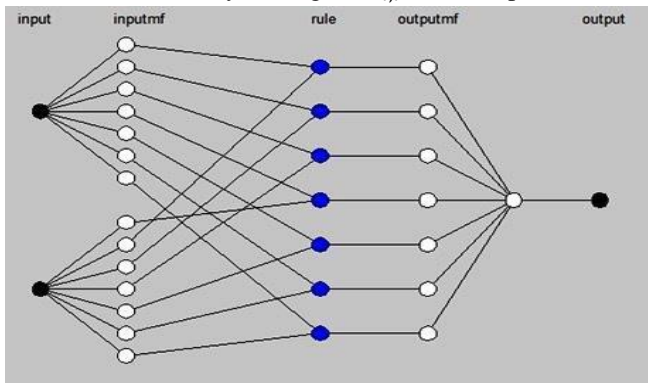


Fig. 6. Structure of the Neuro-Fuzzy control

**Layer 1:**  $x$  and  $y$  are the inputs to the layer 1 nodes having linguistic labels NL, NM, NS, Z, PS, PM, PL. The output of the  $i^{th}$  node in first layer is given as

$$O_{1,i} = \mu_A(x). \quad (12)$$

**Layer 2:** The nodes in this layer are shown with blue color in Fig.6. The output of nodes in the second layer is product of the incoming signals i.e.

$$O_{2,i} = \mu_A(x) \cdot \mu_B(x) \quad (13)$$

Each node in the second layer represent the fire strength of the rule  $i$ .

**Layer 3:** The  $i^{th}$  node in this layer calculates the ratio of firing strength for the  $i^{th}$  rule to the sum of all firing strength, i.e.

$$O_{3,i} = \bar{w}_i = \frac{w_i}{w_1 + w_2 + w_3 + \dots + w_n}. \quad (14)$$

**Layer 4:** In this layer, each node evaluates the fuzzy rule by using output parameter  $p$  and  $q$ . The output of one of the  $i^{th}$  rule, out of  $n$  number of rules in this layer is given as,

$$O_{4,i} = \bar{w}_i \cdot f_i = \frac{w_i}{\sum_{i=1}^n w_i} (p_i x + q_i y + r_i), \quad (15)$$

where  $i = 1$  to  $n$ . Parameter  $p_i, q_i$  and  $r_i$  are known as consequent parameters for the output  $f_i$ .

**Layer 5:** The single node in the 5<sup>th</sup> layer is fixed node which evaluates the overall output as the summation of all incoming signals.

$$O_{5,1} = \sum_i \bar{w}_i \cdot f_i = \sum_i \frac{w_i}{\sum_{i=1}^n w_i} \cdot f_i \quad (16)$$

node in the layer  $l$ .

The fuzzy rule  $f_i$  is stated with linguistic label  $A_i$  and  $B_i$  as,

Rule  $R_i$ : If  $x$  is  $A_i$  and  $y$  is  $B_i$  then  $f_i = p_i x + q_i y + r_i$ .

A Neuro-Fuzzy controller is trained using training data, which can be obtained using practical measurement or another simulation program. Checking data is used to avoid over fitting. The number of samples used for training the controller are given below

TABLE II  
PARAMTERS FOR TRAINING THE CONTROLLER

Parameter	Value
Training data samples	1547000
Checking data samples	1547000
Number of epochs	25

A hybrid learning algorithm is used to modify the parameters of fuzzy sets. The RMS error between training data and controller output is reduced as the number of epochs increase during the training process (Fig. 7).

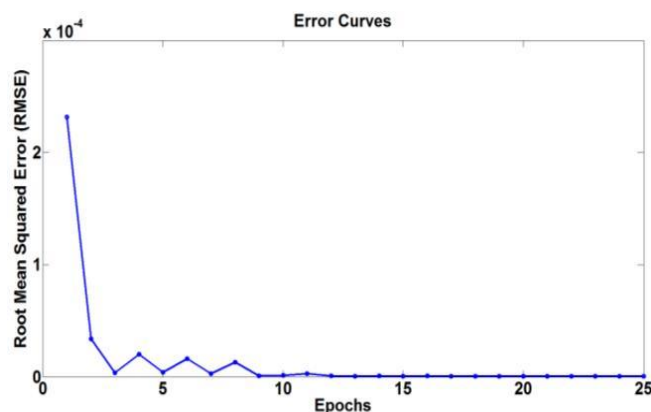


Fig. 7. Structure of the Neuro-Fuzzy control

With each one of seven fuzzy sets for input  $x$  and  $y$ , fuzzy rules are associated. In all, the Neuro-Fuzzy controller makes use of seven rules. The advantage of Neuro-Fuzzy controller is that it uses the minimum number of fuzzy rule set. The training error converged after ten epochs; therefore the Neuro-Fuzzy controller can be trained with fewer epochs for given training samples (Fig. 7).

## VI. SIMULATION RESULTS

The reactor transfer function is obtained at various power levels.

For 100 % rated power,

$$\frac{\Delta P}{\Delta \rho} = \frac{2500 s^7 + 1.21 \times 10^4 s^6 + 1.615 \times 10^4 s^5 + 7619 s^4 + 1509 s^3 + 122.2 s^2 + 3.366 s + 0.02566}{s^8 + 153.2 s^7 + 720.8 s^6 + 951.9 s^5 + 448.7 s^4 + 89.17 s^3 + 7.193 s^2 + 0.196 s + 0.001481}$$

For 80 % rated power,

$$\frac{\Delta P}{\Delta \rho} = \frac{2500 s^7 + 1.211 \times 10^4 s^6 + 1.617 \times 10^4 s^5 + 7638 s^4 + 1515 s^3 + 122.8 s^2 + 3.386 s + 0.02582}{s^8 + 150.8 s^7 + 709 s^6 + 935 s^5 + 439.6 s^4 + 87.09 s^3 + 7.009 s^2 + 0.1907s + 0.00144}$$

For 60 % rated power,

$$\frac{\Delta P}{\Delta \rho} = \frac{2500 s^7 + 1.211 \times 10^4 s^6 + 1.618 \times 10^4 s^5 + 7657 s^4 + 1522 s^3 + 123.5 s^2 + 3.406 s + 0.02597}{s^8 + 147 s^7 + 690.4 s^6 + 908.9 s^5 + 426.1 s^4 + 84.13 s^3 + 6.753 s^2 + 0.1834 s + 0.001384}$$

For 40 % rated power,

$$\frac{\Delta P}{\Delta \rho} = \frac{2500s^7 + 1.212 \times 10^4 s^6 + 1.621 \times 10^4 s^5 + 7685 s^4 + 1531s^3 + 124.4s^2 + 3.434s + 0.02619}{s^8 + 140.1s^7 + 656.6s^6 + 862.8 s^5 + 403.2s^4 + 79.36s^3 + 6.352s^2 + 0.1722s + 0.001298}$$

For 20 % rated power,

$$\frac{\Delta P}{\Delta \rho} = \frac{2500s^7 + 1.212 \times 10^4 s^6 + 1.623 \times 10^4 s^5 + 7710s^4 + 1539s^3 + 125.3s^2 + 3.46s + 0.0264}{s^8 + 123.3s^7 + 574.7s^6 + 752s^5 + 349.5s^4 + 68.38s^3 + 5.444s^2 + 0.1469s + 0.001105}$$

The stability is remarked through Bode plot analysis and Nyquist plot analysis for reactor transfer function at rated power. The Bode plot analysis used to determine how stable the system is by finding gain margin and phase margin (Fig. 8). The Gain cross over frequency (frequency at which gain is 0 db)  $\omega_{gc}$  is 2510 rad/sec. The Phase cross over frequency (frequency where phase shift is equal to  $-180^\circ$ )  $\omega_{pc}$  is ideally infinity. Hence, the Phase Margin (P.M.) can be calculated as P.M. =  $180 - 86.6 = 93.4^\circ$ . The gain margin cannot be determined exactly. As G.M., P.M. are positive &  $\omega_{gc} < \omega_{pc}$ , system is stable. With Nyquist plot, number of poles residing on the right side of the  $j\omega$  axis can be determined. The Fig.9 shows Nyquist plot. The encirclement of  $-1+j0$  point is zero, number of roots of the characteristic equation (the poles of closed loop system) in the right half of the plane is equal to zero, thus system is stable.

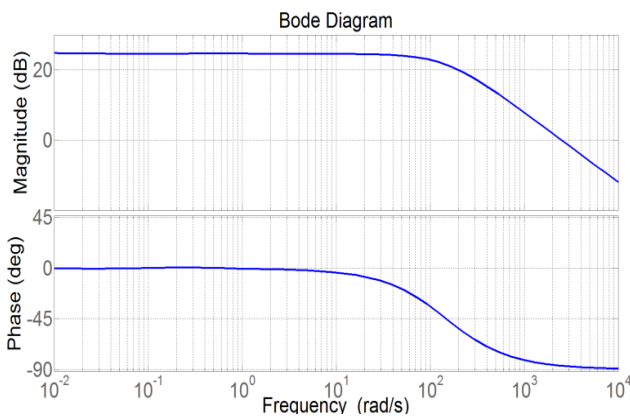


Fig. 8. Bode plot

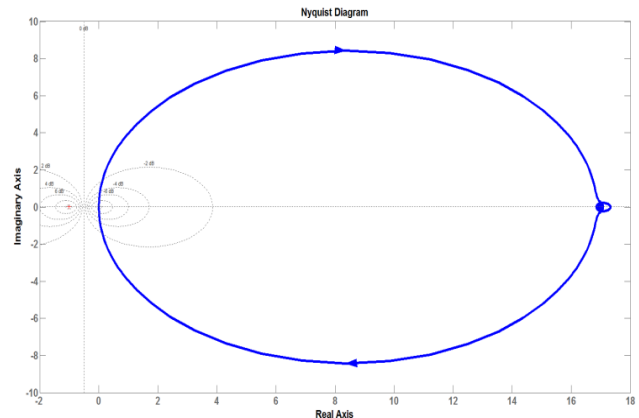


Fig. 9. Nyquist plot

The simulation for load maneuvering operation is accomplished in which external demand is held constant at rated value initially, then it ramps down from 100 s to 500 s, remains constant for next 100 s and then ramps up from 600 s to 1000 s (Fig. 10). The external reactivity fed by the controller is given by Eq. 4. It is function of product of adaptive neuro-fuzzy controller output and reactivity worth of the control rod. The control rod speed is bounded to avoid reactivity excursion by the control rod. The reactor power apparently follows the same trend as that of external demand (Fig. 10), but has small undershoot at 500 s (Fig. 11). The Xenon feedback reactivity (Fig. 12) and feedback power coefficient of reactivity (Fig. 13) were calculated. Any reduction in power increases the Xenon concentration  $[X_e]$  because power reduction decreases the rate at which this nuclide is burned up.  $[X_e]$  reached a maximum at 600 s and decreased further as power increased. The xenon reactivity followed the opposite trend to that of  $[X_e]$ , and had minimum feedback reactivity at 600 s. The feedback power coefficient

of reactivity followed the opposite trend to that of external demand with delay (Fig. 13).

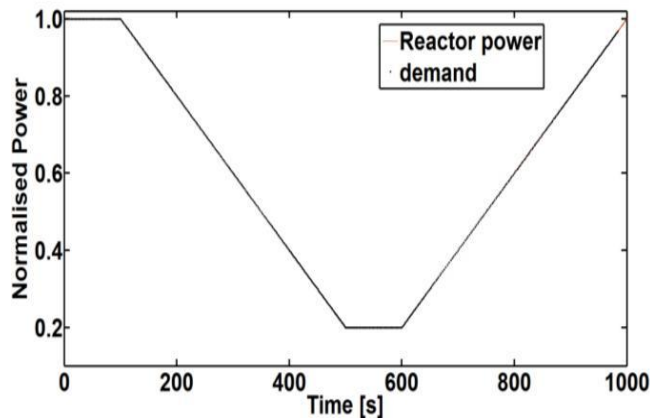


Fig. 10. Load maneuvering operation

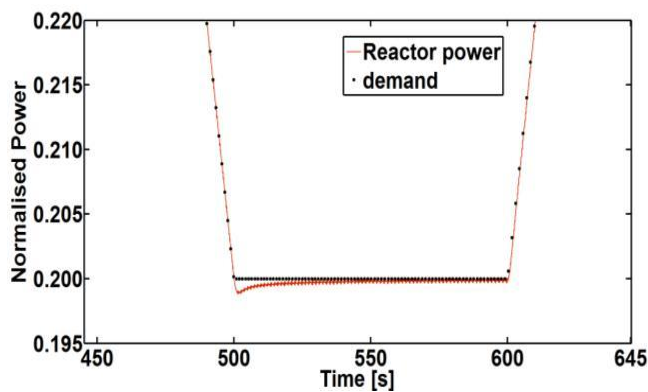


Fig. 11. Load maneuvering operation (Enlarged view)

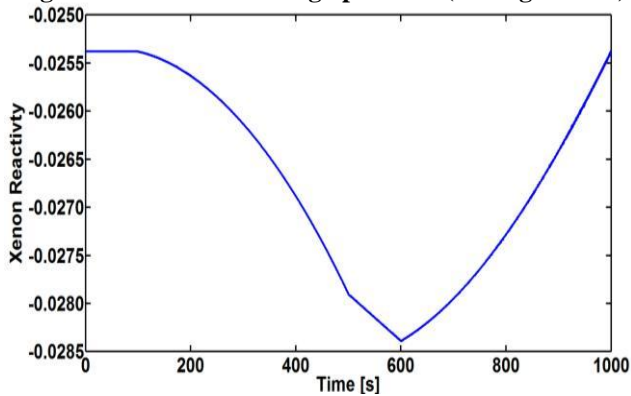


Fig. 12. Xenon feedback reactivity

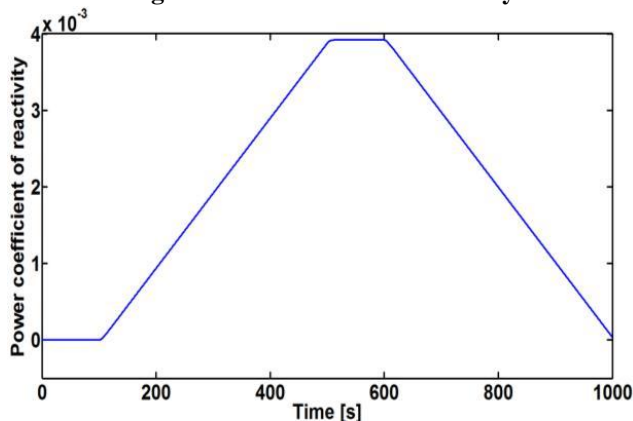


Fig. 13. Feedback power coefficient of reactivity

The RMS error between the normalised reactor power output and external demand was observed (Table III) for the interval of 1000 s in two cases: the first case used the PD controller; the second case used the designed Neuro-Fuzzy controller.

TABLE III  
THE COMPARISON OF THE ERROR

Case	RMS error between normalised reactor power output and demand	Value
1	With PD controller	$7.1016 \times 10^{-4}$
2	With Neuro-fuzzy controller	$6.9 \times 10^{-4}$

These results demonstrate that the proposed Neuro-Fuzzy controller controls the power more accurately than the convention PD controller. The advantage of a Neuro-Fuzzy controller is that it uses the fewer rules than other fuzzy-logic based controllers [6,7,14]. The rule set used by Li and Gatland uses more number of rules; therefore the Neuro-Fuzzy controller is faster in execution. In contrast to online Neural Network learning processes, the Neuro-Fuzzy controller is trained offline. This eliminates the online processing when the controller is connected with the plant. The method has been established using a point kinetics model.

VII. CONCLUSION

This study quantified the design of a Neuro-Fuzzy controller to control the power level in an HTPBR. A simplified reactor model with point kinetics equation and lumped model of heat transfer was developed and used. Xenon feedback and feedback arising from the power coefficient of reactivity were considered. The adaptive Neuro-Fuzzy controller could more precisely control the reactor power with faster execution than can other conventional controllers.

ACKNOWLEDGMENT

This work was supported by World Class University program through the National Research Foundation of Korea funded by the Ministry of Education, Science and Technology (R31-30005).

REFERENCES

1. D. Ruan. (1995 Aug.). Fuzzy logic in the nuclear research world. *Fuzzy Sets and Systems*, 74 (1), pp. 5-13. <http://www.sciencedirect.com/science/article/pii/016501149500020L>
2. D. Ruan. (1998 Mar.). Intelligent systems in nuclear applications. *Int. J. of Intelligent Systems*, 13 (2/3), pp. 115-125. [http://onlinelibrary.wiley.com/doi/10.1002/\(SICI\)1098-111X\(199802/03\)13:2/3%3C115::AID-INT2%3E3.0.CO;2-2/abstract](http://onlinelibrary.wiley.com/doi/10.1002/(SICI)1098-111X(199802/03)13:2/3%3C115::AID-INT2%3E3.0.CO;2-2/abstract)
3. F. Adda, C. Larbes, M. Allek, M. Loudn, 2005. Design of an intelligent fuzzy logic controller for a nuclear research reactor. *Progress in Nuclear Energy*, 46 (3/4), pp. 328-347. <http://www.sciencedirect.com/science/article/pii/S0149197005000296>

4. C. Liu, J. Peng, F. Zhao, C. Li. (2009, Nov.). Design and optimization of fuzzy-PID controller for the nuclear reactor power control. *Nucl. Eng. Des.*, 239 (11), pp. 2311–2316. <http://www.sciencedirect.com/science/article/pii/S0029549309003215>
5. A. P. Tiwari, B. Bandyopadhyay, G. Govindarajan, (1996, Aug.). Spatial control of a large pressurized heavy water reactor. *IEEE Trans. Nucl. Sci.*, 43(4), pp. 2440-2453. <http://ieeexplore.ieee.org/stamp/stamp.jsp?tp=&arnumber=531794>
6. H.M. Emara, A. Elsadat, A. Bahgat, and M. Sultan, (2002, May), "Power stabilization of nuclear research reactor via fuzzy controllers", Proceedings of the American Control. [Online]. Available: <http://ieeexplore.ieee.org/stamp/stamp.jsp?tp=&arnumber=1025469>
7. P.S. Londhe, B.M. Patre, A.P. Tiwari. (2014, Jul.). Fuzzy-like PD controller for spatial control of advanced heavy water reactor. *Nucl. Eng. Des.*, 274, pp. 77–89. <http://www.sciencedirect.com/science/article/pii/S0029549314002362#>
8. X.K. Wang, X.H. Yang, G. Liu, H. Qian. (2009, Jul.), "Adaptive neuro-fuzzy inference system pid controller for sg water level of nuclear power plant", Proceedings of the Eighth International Conference on Machine Learning and Cybernetics. [Online]. Available: <http://ieeexplore.ieee.org/stamp/stamp.jsp?tp=&arnumber=5212517>
9. M. N. Khajavi, M. B. Menhaj, A.A. Suratgar, "Fuzzy adaptive robust optimal controller to increase load following capability of nuclear reactors", International Conference on Power System Technology PowerCon 2000. [Online]. Available: <http://ieeexplore.ieee.org/stamp/stamp.jsp?tp=&arnumber=900041>
- a. K.D. Badgujar, O.P. Singh, S. Singh, S. T. Revankar. (2012, Jul.), "Power Coefficient of Reactivity Determination for HTPBR and Its Application for Reactivity Initiated Transients", Proceedings of the 20<sup>th</sup> ICONE POWER2012, ICONE20POWER2012-55058. [Online]. Available: <http://proceedings.asmedigitalcollection.asme.org/proceeding.aspx?articleid=1762248>
10. [11] K. D. Badgujar, S. T. Revankar, J. C. Lee, M. H. Kim. (2012, Oct.), "Design of fuzzy-PID controller for high temperature pebble bed reactor", *Trans. of the Korean Nuclear Society*, [Autumn Meeting Gyeongju, Gyeongsang, Korea]. [Online]. Available: [http://www.kns.org/kns\\_files/kns/file/30Kushal.pdf](http://www.kns.org/kns_files/kns/file/30Kushal.pdf)
11. K. D. Badgujar, S. T. Revankar, (2013, Jul.), "Design of fuzzy-pid controller for hydrogen production using HTPBR", Proceedings of the 21st ICONE POWER2013, ICONE21-15037. [Online]. Available: <http://proceedings.asmedigitalcollection.asme.org/proceeding.aspx?articleid=1829534>
12. K. D. Badgujar, "Studies on Dynamics of High Temperature Pebble Bed Reactor", M.S. thesis, NETP, IIT Kanpur, Uttar Pradesh, India (April 2009).
13. Li, H., Gatland, H., (1996, Oct.). Conventional fuzzy control and its enhancements. *IEEE Trans. Syst. Man Cybern.*, B 26 (5), pp.791–797. <http://ieeexplore.ieee.org/stamp/stamp.jsp?tp=&arnumber=537321>

University of Science and Technology, Korea. His research interest include simulation and control of electrical machines and motion control application of electrical drives.

## AUTHORS PROFILE



**K. D. Badgujar**, received his Bachelor of engineering from university of Pune. He obtained industrial experience from Diebold, ATM manufacturing company.

He received Master of Technology, from Indian Institute of Technology, Kanpur (IITK), India. He is pursuing his PhD from POSTECH, South Korea, Korea. He has five publications.



**W. M. Lemma**, obtained B.Sc. degree in Electrical Engineering from Arba Minch University, Ethiopia in 2004 and M.Tech from Indian Institute of Technology Delhi, India in 2009. Since 2004 he is a faculty member in Electrical Engineering department, Arba Minch University. He worked also as an associate registrar of Engineering faculty, student service center coordinator and Technical

Manager of Solar Project, Arba Minch Institute of Technology, Arba Minch, Ethiopia. Currently Ph.D. student in Electrical Engineering, Pohang